# A Novel Integrated PCA and FLD Method on Hyperspectral Image Feature Extraction for Cucumber Chilling Damage Inspection

X. Cheng, Y. R. Chen, Y. Tao, C. Y. Wang, M. S. Kim, A. M. Lefcourt

**Abstract.** *High−resolution hyperspectral imaging (HSI) provides an abundance of spectral data for feature analysis in image processing. Usually, the amount of information contained in hyperspectral images is excessive and redundant, and data mining for waveband selection is needed. In applications such as fruit and vegetable defect inspections, effective spectral combination and data fusing methods are required in order to select a few optimal wavelengths without losing the crucial information in the original hyperspectral data. In this article, we present a novel method that combines principal component analysis (PCA) and Fisher's linear discriminant (FLD) method to show that the hybrid PCA−FLD method maximizes the representation and classification effects on the extracted new feature bands. The method is applied to the detection of chilling injury on cucumbers. Based on tests on different types of samples, results show that this new integrated PCA−FLD method outperforms the PCA and FLD methods when they are used separately for classifications. This method adds a new tool for the multivariate analysis of hyperspectral images and can be extended to other hyperspectral imaging applications for fruit and vegetable safety and quality inspections.*

***Keywords.*** *Classification, Dimensionality reduction, Feature extraction, FLD, Hyperspectral imaging, Hyperspectral sensing, PCA, Principal component.*

Chilling damage to produce such as cucumbers usually happens when the produce is stored at low temperatures. The primary cause of the chilling damage is thought to be the injury of plant cell membranes (Saltveit and Morris, 1990). Chilling damage is a result of low temperature over time. Usually, chilling injury can be recoverable if the produce stays below the critical temperature for only a short period of time. But if exposure to the low temperature is prolonged, the damage is irreversible. Detection of chilling damage is difficult, especially at its early stages. The symptoms of injury usually develop after the produce is placed in a warmer environment. Sometimes symptoms develop slowly and are difficult to detect visually. In order to find an effective way to detect chilling injury for automated inspection of fruit and vegetables, a hyperspectral imaging method is used.

Article was submitted for review in September 2003; approved for publication by the Information & Electrical Technologies Division of ASAE in May 2004.

Mention of company or trade names is for purpose of description only.

The authors are **Xuemei Cheng,** Graduate Student, and **Yang Tao, ASAE Member Engineer,** Professor, Department of Biological Resources Engineering, University of Maryland, College Park, Maryland; **Chien Y. Wang,** Horticulturist, Produce Quality and Safety Laboratory, USDA−ARS Beltsville Agricultural Research Center, Beltsville, Maryland; and **Yud−Ren Chen, ASAE Member Engineer,** Research Leader, **Moon S. Kim,** Research Scientist, and **Alan M. Lefcourt, ASAE Member Engineer,** Research Physicist, Instrumentation and Sensing Laboratory, USDA−ARS Beltsville Agricultural Research Center, Beltsville, Maryland. **Corresponding author:** Yang Tao, 1426 Animal Science/Biological Resources Engineering Building, University of Maryland, College Park, MD 20742; phone: 301−405−1189; fax: 301−314−9023; e−mail: ytao@umd.edu.

Hyperspectral sensors have been used to sample the spectral reflectance from objects. The rich spectral response provides sufficient information to identify the spectral reflection peaks and absorbing troughs of materials (Shaw and Manolakis, 2002). The entire spectral region used for sensing spans from the visible region through the near−infrared is divided into hundreds of narrow and contiguous bands. The spectral interval can be as narrow as a few nanometers in wavelength. As a result, over 100 spectral bands or channels are usually used at the same time. By adding a dimension of spectral information to two−dimensional spatial images, hyperspectral data can be perceived as a three−dimensional data cube. Recently, hyperspectral imaging has become a powerful tool and is of enormous interest to researchers in fruit safety and quality inspection. Kim et al. (2001) established a laboratory−based hyperspectral imaging system combining the features of imaging and visible/near−infrared (Vis/NIR) spectroscopy to simultaneously acquire spectral and spatial information for various food commodities, and Kim et al. (2002a, 2002b) used hyperspectral imaging methods for fecal contamination detection on apples. Heitschmidt (1998) used hyperspectral analysis for fecal contamination of poultry products, and Chen et al. (1998), Park et al. (2002), and Windham et al. (2001) showed methods of using hyperspectral imaging for detecting contamination of chicken carcasses.

Lu and Chen (1998) and Lu et al. (1999) found that only two or three essential spectral bands were required for on−line imaging applications to extract unwholesome conditions in food products. Hyperspectral imaging is used as a research tool to determine those essential bands. All the spectral data are studied. Band selection and combination strategies are applied. Since two or three spectral bands for

limited short−time inspection are usually required for commercial applications, the validity of the band−selection and combination strategy for hyperspectral sensing research becomes important. The selected essential bands should not only maintain any valuable details that are needed, but also simplify the successive discrimination and classification procedures. This research is focused on developing a band combination method that can be applied to hyperspectral research on fruit and vegetable inspection.

A hyperspectral image cube can be considered as a high−dimensional feature space. Each feature is represented as a spectral image, and the reflection properties from wholesome and unwholesome objects are associated as different patterns. The hyperspectral band selection problem can then be viewed as a feature extraction problem in statistical pattern recognition. The well−known linear transforms or projection pursuit methods for feature extraction and dimensionality reduction are principal component analysis (PCA) and linear discriminant analysis (LDA). PCA is widely used in fecal−contaminated apple inspection (Kim et al., 2002a, 2002b) and other fruit and vegetable quality and safety inspections. However, Talukder and Casasent (1998) point out that PCA, as an unsupervised method, is not necessarily good at drawing distinctions between patterns. In this article, the objective is to present a new method that combines the PCA method and Fisher's linear discriminant (FLD) method to aid in the criteria development for selecting spectral bands for multispectral imaging applications. This new method and the individual PCA and FLD methods are each applied to cucumber chilling injury inspection. The detection results obtained by using the new method are presented and compared with PCA and FLD, respectively.

## Materials and Method

### Sample Materials

Cucumbers were freshly picked from a farming field. Ninety cucumbers were divided into 30 groups of 3 cucumbers each. Each group was placed in a plastic bag punched with holes to allow for air circulation. In temperature−controlled cold storage rooms, 15 of the bags were stored at 0˚C, and the other 15 were stored at 5˚C. On each day over a period of 15 days, one bag was moved from each cold storage room to an air−conditioned laboratory at 18˚C to 20˚C. Each day, hyperspectral images were collected for the 6 (two groups of 3) newly moved cucumbers and for all the cucumbers previously moved from cold storage. The last two groups were moved after 15 days in cold storage, and image collection continued for 6 days afterwards. Chilling injury was categorized into four different damage levels: trace, slight, moderate, and severe. For cucumbers stored at 0˚C, symptoms of trace chilling injury first appeared on cucumbers that had spent 4 days in cold storage and then 2 days at room temperature. For cucumbers stored at 5˚C, symptoms of trace chilling injury first appeared on cucumbers that had spent 5 days in cold storage and 1 day at room temperature. Early trace and slight chilling injury was observed. Some cucumbers that showed early trace and slight levels of chilling damage subsequently appeared to recover after several days at room temperature. Typical samples of these injury levels are shown in figure 1.

A large degree of variation in both color and skin smoothness can exist between individual cucumbers. These natural differences increase the difficulty of detecting chilling damage even during the human visual inspection process. For instance, bumpy−skinned cucumbers can be easily mistaken to have trace or slight chilling damage due to the visual similarities, as shown in figure 2. This became the most challenging part of our experiment for effective detection. The cucumber samples also varied in size and shape in their hyperspectral images. In order to keep the input data consistent, only a portion of each cucumber image was used for the input image samples. The binning size of the region of interest was 45 × 45 pixels. This size covered the average spot area of chilling damage. For an individual cucumber sample, different levels of chilling injury may appear on different portions of the cucumber skin and thus may produce different image samples for training or testing purposes. Data collected for the 90 cucumber samples during three weeks' time provided a huge number of input image samples. Moreover, since the cucumbers developed different types of chilling injuries unevenly, different numbers of samples were chosen for training and testing of the algorithms, as summarized in table 1. Three experiments were

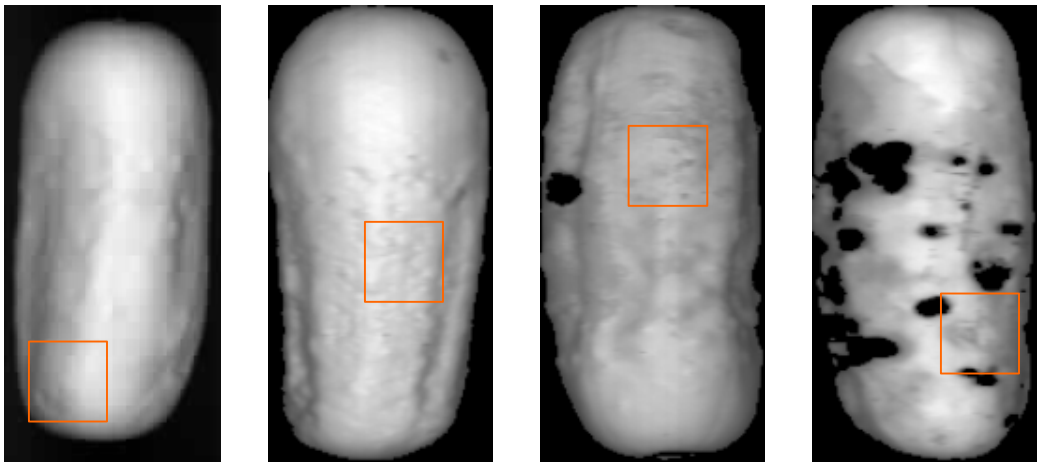

(a) Trace (b) Slight (c) Moderate (d) Severe

**Figure 1. Four levels of chilling injury (presented in the rectangular area) of cucumbers detected in this study: (a) trace chilling injury, (b) slight chilling injury, (c) moderate chilling injury, and (d) severe chilling injury. All images were taken at 800 nm (near−infrared).**

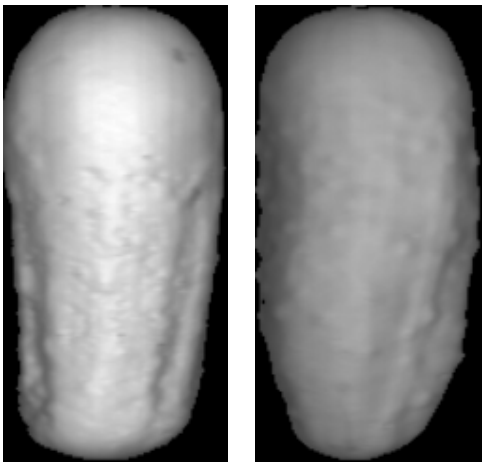

**(a) slight chilling damaged cucumber** **(b) bumpy good cucumber**

**Figure 2. NIR reflectance images of: (a) a cucumber with slight chilling damage, and (b) a healthy cucumber with bumpy skin. The two images show the similarity in appearance of the two cucumbers. The images were taken at 800 nm.**

conducted on testing different methods with different types of cucumber samples.

### Hyperspectral Sensing System

A laboratory−based hyperspectral sensing and imaging system established by the USDA Instrumentation and Sensing Lab (ISL) was used to scan each sample. For a detailed description of this equipment, refer to Kim et al. (2001, 2002a). In this study, only reflectance measurements were analyzed. The illumination for reflectance imaging was provided by two 150 W halogen lamps. The equipment was operated in a line−by−line scan mode at a line length of 460 pixels. The scanned wavelengths ranged from 447.3 nm to 951.2 nm with a 4.5 nm interval, for a total of 112 spectral bands. Once a single line was scanned, a 112 × 460 (spectral by spatial) pixel image was generated. Due to the maximum length of the cucumber samples, 300 lines were accumulated for each cucumber. During the scanning process, the system was operated in a darkened room to prevent interference from ambient light.

Each pixel value in the 1 × 112 spatial−by−spectral image was proportional to the reflectance factor of the sample at that pixel position. The reflectance factor was defined by dividing the reflection radiation intensity at each pixel position of a sample by that of a known reference under the same illumination situation. For system calibration, a white Spectralon panel (Labsphere, Inc.) with nearly 99% reflection ratio was used as the reference. To obtain a proper dynamic range of the image data, the reflectance factors were expanded by a fixed number and then assigned to be the pixel values of the spatial by spectral image.

**Table 1. Cucumber sample diversity.**

| Class | Total Number | Type of Cucumber | Sample Number |
|---|---|---|---|
| Defective Cucumbers | 140 | Trace | 20 |
| | | Slight | 50 |
| | | Moderate | 35 |
| | | Severe | 35 |
| Good Cucumbers | 140 | Good with bumpy skin | 90 |
| | | Good smooth | 50 |

### Feature Extraction with Integrated PCA−FLD Method

Principal component analysis (PCA), also known as the Karhunen−Loeve transform, uses orthogonal axes for dimensionality reduction by performing an eigen−decomposition of the covariance matrix of the data. Let $\Sigma$ represent the covariance matrix; $\Sigma$ can then be obtained by (Johnson, 1998):

$$\Sigma = \frac{1}{n-1}\sum_{k=1}^{n}(\mathbf{x}_k - \mu)(\mathbf{x}_k - \mu)^T \quad (1)$$

where $\mu$ is the mean vector of a pixel set, $\mathbf{x}_k$ represents the $k$th random sample of a band vector with a dimension of N (where N represents the number of feature bands), and $n$ is the sample size of $\mathbf{x}_k$. The dimension of $\Sigma$ is N × N. Based on the variance−covariance matrix ($\Sigma$), a total scatter matrix ($\mathbf{S}_t$) is defined as: $\mathbf{S}_t = (n - 1) * \Sigma$ (Belhumeur et al., 1997). The eigen−decomposition transform is to maximize the energy of the projected samples, denoted as:

$$E_{pca} = \phi_m^T \mathbf{S}_t \varphi_m \quad (2)$$

where $\phi_m$ is one of the transform vectors used to project the data samples, and $m$ = 1 ... N. By performing the eigen−decomposition of the total scatter matrix, it can be demonstrated that the transformed data compared with the original data has minimized the mean square error. The magnitude of the eigenvalue indicates the energy residing in the data along the direction parallel to the corresponding eigenvector. The larger the eigenvalue, the higher the energy it represents. Hence, to reduce the original N−dimensional data to a lesser dimension (M), one can project the original data to the M eigenvectors corresponding to the largest M eigenvalues. By taking the first few significant compositions, this transform results in a lower−dimensional multivariate feature vector that still preserves most of the energy in the original N−dimensional system.

Fisher's linear discriminant (FLD) method is an effective, class−specific method that projects the scatter of data to make them more reliable for classification. Two matrices are introduced in the FLD: one is the between−class scatter matrix ($\mathbf{S}_b$), and the other is the within−class scatter matrix ($\mathbf{S}_w$). The between−class scatter matrix ($\mathbf{S}_b$) is defined as (Belhumeur et al., 1997):

$$\mathbf{S}_b = \sum_{i=1}^{c}|\chi_i|(\mu_i - \bar{\mu})(\mu_i - \bar{\mu})^T \quad (3)$$

and the within−class scatter matrix ($\mathbf{S}_w$) is defined as:

$$\mathbf{S}_w = \sum_{i=1}^{c}\sum_{\mathbf{x}_k \in \chi_i}(\mathbf{x}_k - \bar{\mu}_i)(\mathbf{x}_k - \bar{\mu}_i)^T \quad (4)$$

where $\bar{\mu}_i$ is the mean of class $i$, $\bar{\mu}$ is the mean of the total samples, $c$ is the number of classes, $\chi_i$ represents the $i$th class, and $|\chi_i|$ is the number of samples in class $i$. The optimal data projection can be obtained by choosing the transform vectors ($\phi_m$) that maximize the ratio of the projected between−class samples to the projected within−class samples ($E_{fld}$), defined as:

$$E_{fld} = \frac{\sum_{m=1}^{M}\phi_m^T \mathbf{S}_b \phi_m}{\sum_{m=1}^{M}\phi_m^T \mathbf{S}_w \phi_m} \quad (5)$$

Note that the PCA method does not guarantee the representation of the feature class separability of the selected band. On the other hand, the FLD method, although it is effective in class segmentation, is sensitive to noise and may not convey enough energy from the original data.

In order to design a set of transform vectors that can provide supervised classification information well, and at the same time, preserve enough energy from the original data cube, a new method is proposed to combine equations 1 through 4 to construct an evaluation equation, which is called the integrated PCA−FLD method. A weight factor ($K$) is introduced to adjust the degree of classification and energy preservation as desired. The constructed evaluation equation is given as:

$$E_{evl} = \sum_{m=1}^{M} \frac{\phi_m^T [K\mathbf{S}_t + (1-K)\mathbf{S}_b]\phi_m}{\phi_m^T [K\mathbf{I} + (1-K)\mathbf{S}_w]\phi_m} \quad (6)$$

where $K \in [0,1]$, and $\mathbf{I}$ is the identity matrix. In equation 5, if the within−class scatter matrix ($\mathbf{S}_w$) becomes very small, the eigen−decomposition becomes inaccurate. Equation 6 overcomes this problem. If the previous situation happens, by adjusting the weight factor $K$ toward 1, the effects of $\mathbf{S}_w$ can be ignored, which means the principal components are more heavily weighted. On the other hand, if the $K$ value chosen is small, which means more differential information between classes is taken into effect, then the ratio between $\mathbf{S}_b$ and $\mathbf{S}_w$ dominates. The integrated method magnifies the advantages of PCA and FLD and compensates for the disadvantages of the two at the same time.

In fact, the FLD and PCA methods represent the extreme situations of equation 6. When $K = 0$, only the discrimination measure is considered, and the equation is in fact equal to FLD (eq. 5). If $K = 1$, only the representation measure is important, and the evaluation equation is equivalent to the PCA method (eq. 2). To find the transform that works equally well on representation and discrimination, one can find the set of $\phi_m$ that maximizes equation 6 where $K = 0.5$. The solution of $\phi_m$ is called the generalized eigenvector, which is obtained by setting the derivative of equation 6 with respect to $\phi_m$ to be zero. We have:

$$\left[\frac{K\mathbf{S}_t + (1-K)\mathbf{S}_b}{K\mathbf{I} + (1-K)\mathbf{S}_w}\right]\phi_m = \lambda_m \phi_m \quad (7)$$

where $\lambda_m$ represents the eigenvalues, and $\phi_m$ is the corresponding generalized eigenvector.

For the hyperspectral dimensionality reduction, suppose that the original feature space is N−dimensional. The reduced M (M < N) dimensional features can then be formed by selecting the M generalized eigenvectors corresponding to the M largest eigenvalues obtained from equation 7. Note that the $K$ value changes between 0 to 1, which shifts the weight between PCA and FLD. For a given $K$ value, a maximized $E_{evl}$ (eq. 6) is supposed to give an optimal projection on the original feature space. The projected samples become the best in representation and classification at the proportion determined by $K$. For any application, an optimal proportion between PCA and FLD exists, and by searching the $K$ value from 0 to 1, one can find the optimal $K$ value that achieves the best classification rate of the samples. The changes of the classification rate by different $K$ values will be discussed in the next section.

The transformation matrix $\mathbf{T}$ (N × M) is formed by selecting M generalized eigenvectors as the column vectors in the matrix. The linear transform is defined as:

$$\mathbf{Y} = \mathbf{T}^T\mathbf{X} \quad (8)$$

where $\mathbf{X}$ represents the original feature space with the given N × J dimension (where N represents the features, and J is the sample size), and $\mathbf{Y}$ is the transformed feature space with M × J dimension. $\mathbf{Y}$ is the new features (or bands) that were obtained from the linear combination of all the original features/bands. Since $\mathbf{T}$ consists of M eigenvectors that correspond to the M largest eigenvalues, $\mathbf{Y}$ can provide a better classification and representation ability than the M best subsets of given features in $\mathbf{X}$.

In this study, M = 1 is chosen. Only the eigenvector corresponding to the largest eigenvalue of equation 7 is used in the feature extraction. In this case, $\mathbf{Y}$ represents a single feature vector (we call it the first principal feature vector) that is generated by linear combination of the original N features by using the integrated PCA−FLD method. Similarly, by applying the PCA or FLD method individually, one may obtain the first principal feature vector for PCA or FLD, respectively, where in PCA the first principal feature vector is in fact the first principal component. Although the physical meaning of the first principal feature vector in the integrated PCA−FLD method becomes unclear, it may provide the best discriminative feature compared with any individual N features in the original feature space.

All methods mentioned above aim to establish a good transformation matrix to define the similarity or difference among patterns. When the original hyperspectral data cube is transformed, spectral feature vectors are obtained for each image sample selected. A classifier is designed to determine the category of input image samples. For spectral feature vectors that belong to one image sample, both the mean and the standard deviation of the feature vectors are calculated. The ratio of the standard deviation over the mean is used as the numerical input variable to a $k$−nearest neighbor algorithm. The $k$−nearest neighbor algorithm is used to determine the $k$ samples in the training set that are closest to the $x$th unknown sample in the testing set. Because patterns with similar attributes should be assigned to the same class, samples with closer ratios are classified as the same category. Therefore, if a majority of the $k$ nearest neighbors belongs to the good cucumber class, then the $x$th sample is classified as a good cucumber; otherwise, it is classified as an injured cucumber. We used $k = 15$ in the classifier.

## Results and Discussion

Figure 3 shows the averaged reflectance intensity over the wavelength curves for six types of cucumbers. The main difference lay in the visible range from 500 nm to 580 nm, and in the near−infrared range above 700 nm (the visible range represents the color of cucumber pigment). As shown in figure 3, cucumbers with severe and moderate chilling injury had greater absorbance within this spectral range and were easier to distinguish from the wholesome ones. On the other hand, cucumbers with trace or slight damages showed little difference from good cucumbers. In particular, over most of the spectral range, the curves of bumpy−skin good cucumbers were mixed together with those of trace or slightly injured cucumbers. It became much more challenging to differentiate them.

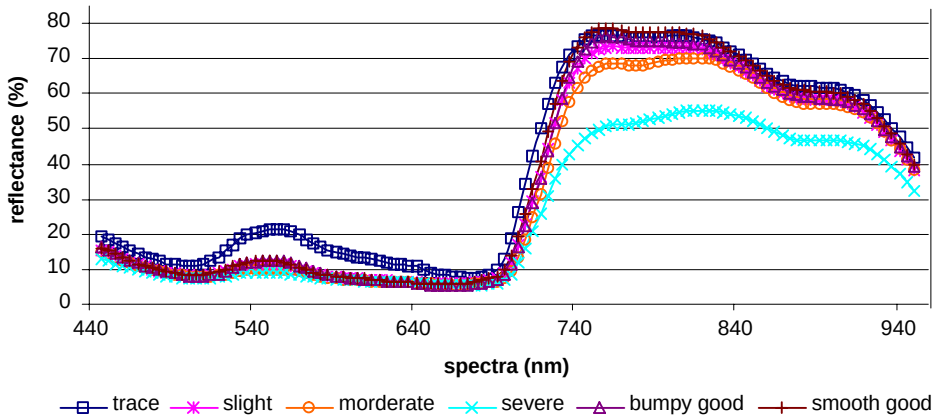


**Figure 3. The hyperspectral reflectance effect on wholesome (bumpy good and smooth good) cucumbers and unwholesome (with chilling injury levels of trace, slight, moderate, and severe) cucumbers.**

In the new method, the *K* value was used to adjust the balance between the representative and classification abilities of the projection matrix, and therefore increased the flexibility of the method. For different image samples, however, the optimal *K* values should differ. An effective method for *K* value selection was needed. In this study, we searched the *K* value from 0 to 1 at a step of 0.05. When the *K* value was changed, the recognition rates varied. As an example, figure 4 shows the sensitivity of *K* value versus the classification rates for two groups in a total four tests using a small set of only 20 image samples. The samples used for the four tests are shown in table 2. The overall classification rate changed gradually over the *K* values. For different samples, the optimal *K* values differed. In the group 1 tests, where the injured cucumbers were easier to distinguish from the good ones, the optimal *K* values were in the range of 0.35 to 0.95. In the group 2 tests, since the two classes of image samples were similar, the optimal *K* values were in the range of 0.05 to 0.60. The overlapping range of optimal *K* values was from 0.35 to 0.60. In most cases in this study, a *K* value in this range gave the best performance. But as shown in figure 4b, in the test for detecting trace−injured cucumbers from bumpy good ones, the optimal *K* value was from 0.05 to 0.25. A *K* value between 0.35 and 0.6 resulted in classification errors.

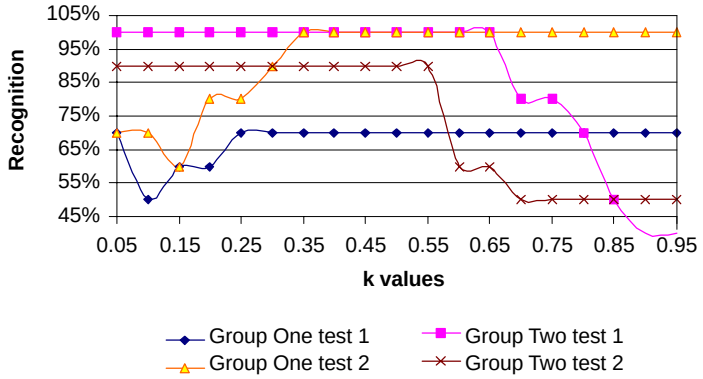


**Figure 4a. Good cucumber recognition rates versus *K* values for four validating tests, where each test used 20 different image samples.**

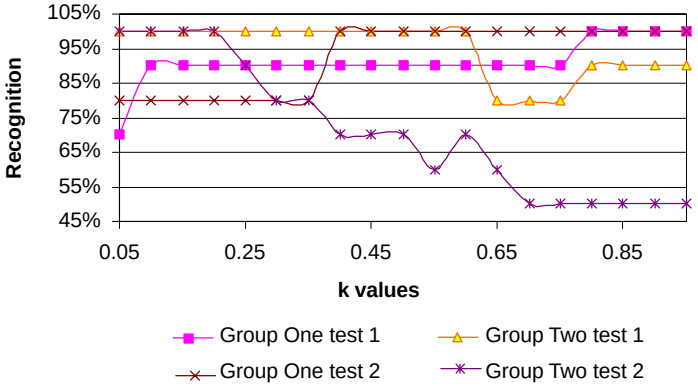


**Figure 4b. Chilling injury detection rate versus *K* values for the same four validating tests shown in figure 4a.**

**Table 2. Samples used for optimal *K* value tests.**

| Group | Test | Type of Cucumber | Number |
|---|---|---|---|
| 1 | Test 1 | Moderate and smooth good | 20 |
| | Test 2 | Severe and smooth good | 20 |
| 2 | Test 1 | Slight and bumpy good | 20 |
| | Test 2 | Trace and bumpy good | 20 |

In general, by choosing optimal *K* values, both the representation and classification effects were properly weighted for the testing samples. The small−set sample tests can be considered a validating process before the training and the testing process. Those image samples were called validating image samples and were used to determine the variable parameters (in our experiments, the optimal *K* value) in the method before final application to the training and testing processes.

The image samples used for these experiments are listed in table 3. In the first experiment, 50 good smooth−skinned cucumber images and 50 injured cucumber images (with moderate and severe degrees of damage) were selected. From among these, 20 good cucumber image samples and 20 injured samples were used for training and then tested together with the remaining 60 samples. The total 100−sample testing results, shown in figure 5, were obtained by choosing an optimal *K* value of 0.60. The result indicated that the PCA method and the integrated PCA−FLD method achieved a similar performance that was better that that of the FLD method. Note that the sample classes used in the first experiment were well separated. The solution was dominated by the principal components. So the PCA method becomes good at classifying data that are well distinguishable, and this is consistent with the results of Kim et al. (2002a, 2002b). On the other hand, for the FLD method, since FLD is intended to maximize the $E_{fld}$ ratio shown in equation 5, which is small in this case, it becomes unreliable and noise sensitive, and led to the poor performance in this situation.

More challenging samples were trained and tested in the second and third experiments, as listed in table 3. The recognition results are shown in figures 6 and 7, respectively. In the second experiment, 60 samples were used for training, and the same samples were used for testing; therefore, the recognition rates for both good and injured cucumbers were high. In this case, the *K* value was set at 0.20. Since these two classes had very similar spectral characteristics, the differentiating information played a more important role in classification. Therefore, the FLD solution showed better performance than PCA. By using the FLD method, the defect recognition rate achieved 90%, and the good sample recognition rate was 100%, which were, respectively, 5% and 2% higher than those achieved with the PCA method.

**Table 3. Samples used for the experiments.**

| Experiment | Sample Type | Sample Number | Training Set | Testing Set |
|---|---|---|---|---|
| 1 | Good smooth | 50 | 20 | 50 |
| | Moderate | 25 | 10 | 25 |
| | Severe | 25 | 10 | 25 |
| 2 | Good with bumpy skin | 30 | 30 | 30 |
| | Trace | 10 | 10 | 10 |
| | Slight | 20 | 20 | 20 |
| 3 | Good with bumpy skin | 60 | 20 | 40 |
| | Trace and slight | 40 | 10 | 30 |
| | Moderate and severe | 20 | 10 | 10 |

In the last experiment, 40 samples were used for training, and an additional 80 samples were tested. The samples were diversified and covered all types of injured cucumbers mentioned before. In this case, the *K* value was set at 0.20. The integrated PCA−FLD method achieved recognition rates of 93.3% for injured cucumbers and 88.3% for good cucumbers. In all experiments, the integrated PCA−FLD method achieved the best recognition results compared with those of the other methods.

Table 4 summarizes the three methods discussed above. All these methods are considered transformation−based feature extraction methods. The original features are linearly combined to produce new projected features at a lower dimension. The new projected features compared with any subset of the original features at the same dimension have a better performance in some aspects. For instance, the new projected features generated by the PCA method are good at pattern representation and at differentiating obviously separated patterns. For similar patterns, the FLD method performs better for classification purposes. However, since the distinguishing information between two classes in FLD is more heavily weighted, FLD is more sensitive to noise and is less stable than PCA. The integrated PCA−FLD method overcomes the drawbacks of these two methods while it preserves the advantages of both. Moreover, the new method provides more flexibility in dealing with different sample patterns by adjusting the *K* value properly.

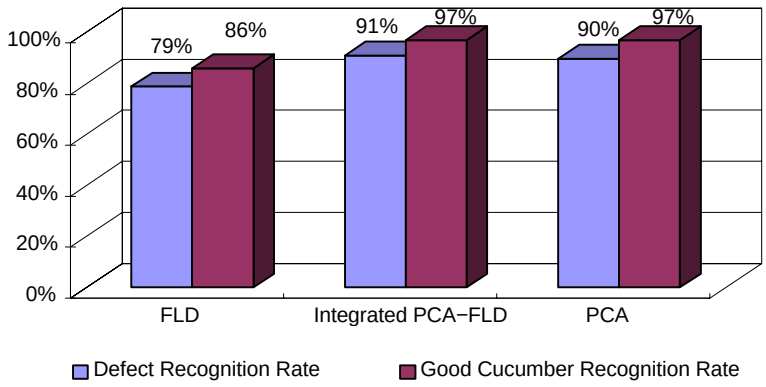


**Figure 5. Chilling injury detection rates and good cucumber recognition rates using FLD, PCA, and integrated FLD−PCA methods for the first experiment, where 20 image samples were used for training and, together with another 80 image samples, were tested. The rates were calculated based on the 100 total testing samples.**

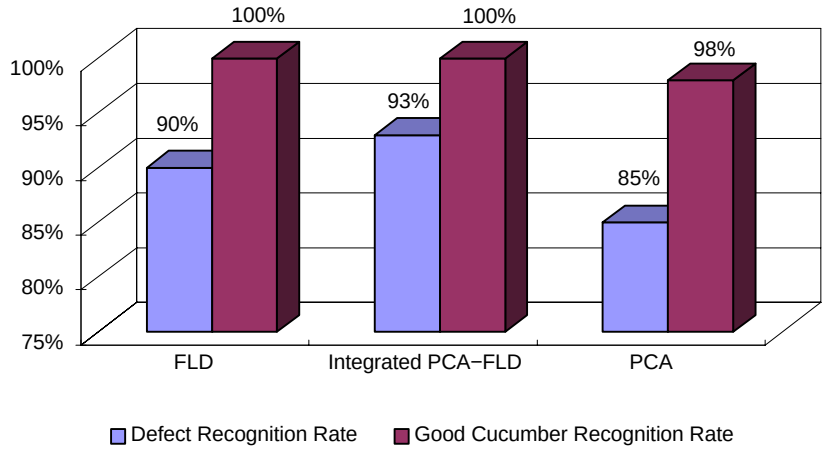


**Figure 6. Chilling injury detection rates and good cucumber recognition rates using FLD, PCA, and integrated FLD−PCA methods for the second experiment, where 60 cucumber image samples were used as training samples and the same 60 image samples were tested.**

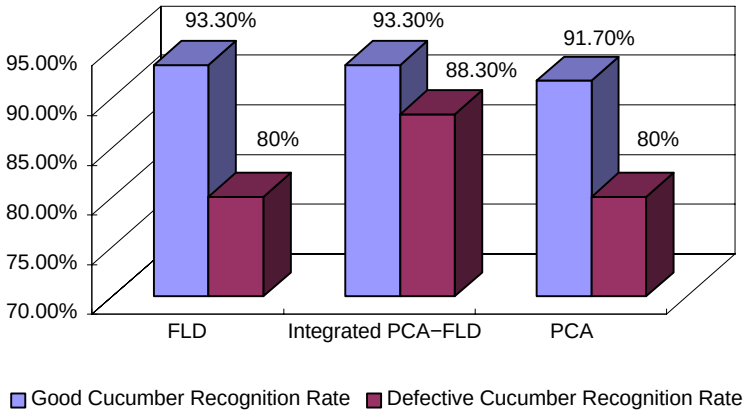


**Figure 7. Chilling injury detection rates and good cucumber recognition rates using FLD, PCA, and integrated FLD−PCA methods for the third experiment, where 40 image samples were used as training samples and another 80 image samples were used as testing samples. The rates were calculated based on the 80 testing image samples only.**

**Table 4. Summary of three feature extraction methods.**

| Method | Property | Comments |
|---|---|---|
| PCA | Linear transform, eigenvector−based | Good representative, good for distinguished data classification. |
| FLD | Linear transform, eigenvector−based | Good for discrimination of similar data classification. |
| Integrated PCA−FLD | Linear transform, eigenvector−based | Good for both representation and discrimination; must choose proper *K* value. |

## CONCLUSIONS

In this study, we proposed a novel integrated PCA−FLD method for hyperspectral feature extraction and applied it to cucumber chilling injury detection. The integration process was neither a simple combination of the two methods nor used them sequentially during the entire procedure. The new method was derived based on a constructed evaluation equation that combined the representation and classification effects together. Based on our sample data, better recognition performance was achieved by using the new method.

We concluded that for hyperspectral band combination, integrated effects of both representation and classification should be taken into account. The principal components preserved the most energy of the original data, and provided good performance in recognizing obviously separated classes. The discriminant analysis contributed to classifying similar patterned classes. By properly adjusting the weight factor (*K*), the integrated PCA−FLD method was more flexible in processing different sample patterns, and the result became robust with respect to noise. This method can be extended to other hyperspectral imaging applications for safety and quality inspections.

### ACKNOWLEDGEMENT

The authors would like to thank Ms. Diane Chan for her cooperation and help in sample preparation and data collection to make this research possible.

## REFERENCES

Belhumeur, P. N., Hespanha, J. P., and Kriejman, D. J. 1997. Eigenfaces vs. Fisherfaces: Recognition using class−specific linear projection. *IEEE Trans. on PAMI* 19(7): 711−721.

Chen, Y. R., B. Park, R. W. Huffman, and M. Nguyen. 1998. Classification of on−line poultry carcasses with backpropagation neural networks. *J. Food Proc. Eng.* 21: 33−48.

Heitschmidt, J., M. Lanoue, C. Mao, and G. May. 1998. Hyperspectral analysis of fecal contamination: A case study of poultry. *SPIE* 3544: 134−137.

Johnson, D. E. 1998. *Applied Multivariate Methods for Data Analysis*, 26−27. 5th ed. Pacific Grove, Cal.: Brooks/Cole.

Kim, M. S., Y. R. Chen, P. M. Mehl. 2001. Hyperspectral reflectance and fluorescence imaging system for food quality and safety. *Trans. ASAE* 44(3): 721−729.

Kim, M. S., A. M. Lefcourt, Y. R. Chen, I. Kim, D. E. Chan, and K. Chao. 2002a. Multispectral detection of fecal contamination on apples based on hyperspectral imagery: Part I. Applications of visible and near−infrared reflectance imaging. *Trans. ASAE* 45(6): 2027−2037.

Kim, M. S., A. M. Lefcourt, Y. R. Chen, I. Kim, D. E. Chan, and K. Chao. 2002b. Multispectral detection of fecal contamination on apples based on hyperspectral imagery: Part II. Applications of hyperspectral fluorescence imaging. *Trans. ASAE* 45(6): 2039−2047.

Lu, R., and Y. R. Chen. 1998. Hyperspectral imaging for safety inspection of food and agricultural products. *SPIE* 3544: 121−133.

Lu, R., Y. R. Chen, B. Park, and K. H. Choi. 1999. Hyperspectral imaging for detecting bruises in apples. ASAE Paper No. 993120. St. Joseph, Mich.: ASAE.

Park, B., K. C. Lawrence, W. R. Windham, and R. J. Buhr. 2002. Hyperspectral imaging for detecting fecal and ingesta contaminants on poultry carcasses. *Trans. ASAE* 45(6): 2017−2026.

Saltveit, M. E., Jr., and L. L. Morris. 1990. Overview on chilling injury of horticultural crops. In *Chilling Injury of Horticultural Crops*, 3−16. C. Y. Wang, ed. Boca Raton, Fla.: CRC Press.

Shaw, G., and D. Manolakis, 2002. Signal processing for hyperspectral image exploitation. *IEEE Signal Processing Magazine* 19(1): 12−16.

Talukder, A., and D. Casasent. 1998. A general methodology for simultaneous representation and discriminant of multiple object classes. *Optical Eng.* (special issue on advances in recognition techniques) 37(3): 904−913.

Windham, W. R., K. C. Lawrence, B. Park, and R. J. Buhr. 2001. Visible/NIR spectroscopy for characterizing fecal contamination of chicken carcasses. ASAE Paper No. 016004. St. Joseph, Mich.: ASAE.